Journal of Chromatography, 550 (1991) 301–312
Elsevier Science Publishers B.V., Amsterdam

CHROMSYMP. 2280

Stationary phase effects in reversed-phase liquid chromatography under overload conditions

N. T. MILLER
Research & Development Center, The PQ Corporation, Conshohocken, PA 19428 (USA)

ABSTRACT

Stationary phase parameters that influence the performance of silica-based reversed phases under overload conditions were examined. High concentrations of the solute 2-phenylethanol were eluted from a variety of C_{18} packings differing in particle diameter and surface area (pore size). Apparent efficiency and retention factors of the solute bands resulting from concentration overload in these systems were measured and compared. In agreement with the literature, beyond a certain solute load and depending on the initial efficiency of the system, the dependence of column efficiency on load is less influenced by the stationary phase particle diameter. Smaller pore (*i.e.*, nominal 100 Å) C_{18} packings showed a slightly greater efficiency and less retention loss with an increase in sample load than larger pore (*i.e.*, nominal 200 Å) sorbents. The small-pore silicas also showed a greater decrease in pore volume relative to large-pore silicas when used as substrates for C_{18} bonding. The chromatographic data could also be used to calculate coefficients of the Langmuir adsorption isotherm. Changes in total porosity of the column greatly influence the determination of the dominant coefficient in the Langmuir equation.

INTRODUCTION

Preparative liquid chromatography continues to develop, as evidenced by increasing interest in international symposia and consolidation of commercial activity. Key advances in the theory of large-scale chromatography [1–4] complement basic studies [5–7]. In particular, the development of a theoretical framework (*i.e.*, the ideal and semi-ideal models) has revealed under-appreciated effects in the elution behavior of large-concentration bands (*i.e.*, competitive adsorption, sample self-displacement [8] and tag-along phenomena [9]), which play a significant role in the optimization of throughput, mass yield and purity. Practical guidelines for optimized preparative separations also exist to benefit the user [10].

The availability of preparative chromatographs and column technology for use with modern microparticulate packings has made the technique more acceptable. Preparative columns now employ compression technology such that 10-μm diameter porous silicas and bonded phases can be used routinely [11,12].

From a practical point of view, much work remains to be done on the optimized use of stationary phases in preparative chromatography, for example, to establish what compromise should be struck between sorbent surface area for sample capacity and sorbent mechanical strength. Although several reports have discussed the role of

0021-9673/91/$03.50

particle characteristics in preparative liquid chromatography, confusion still exists in the literature [13,14]. Sorbent reproducibility and stability will continue to be a concern, as will economics of packing use and reuse.

In this paper, we examine several characteristics of column packings for the elution of a single-solute band at high concentration, including the effect of C_{18} reversed-phase particle diameter and surface area.

EXPERIMENTAL

Equipment

A Perkin-Elmer (Norwalk, CT, USA) liquid chromatograph consisting of a Series 410 solvent delivery pump, a Model ISS-100 autosampler and a Model LC-95 variable-wavelength UV detector was used to obtain elution band profiles. Data were recorded on a Chromatopac C-R6A integrator (Shimadzu, Columbia, MD, USA) and on an IBM-AT computer (IBM, Boca Raton, FL, USA) using Nelson Analytical (Cupertino, CA, USA) chromatography software.

Materials

High-coverage and end-capped IMPAQ reversed-phases were obtained from PQ (Conshohocken, PA, USA) and are listed in Table I with characteristics. The sorbents were slurry-packed into 15 cm × 0.46 cm I.D. columns using a pneumatic-amplifier pump (Haskel, Burbank, CA, USA). Uracil and 2-phenylethanol were obtained from Sigma (St. Louis, MO, USA). Polystyrene of molecular weight $1.8 \cdot 10^6$ was purchased from Supelco (Bellefonte, PA, USA). High-performance liquid chromatographic grade water was prepared in-house. Other solvents were obtained from EM Science (Cherry Hill, NJ, USA).

Procedures

Solutions of 2-phenylethanol in the range 1–600 mg/ml were prepared by weighing the solute into volumetric flasks and diluting to volume with methanol or with the mobile phase ($\leqslant$30% aqueous methanol). Injections of variable sample volumes for a fixed sample concentration were made to determine the onset of volume overloading for a given column. Thereafter, in concentration overload studies, fixed sample volume injections (*e.g.*, 5–20 μl) well under that needed for volume overloading were employed. The detector response was calibrated using step gradients of known solute concentration [15] or a linear solute concentration gradient. Solute concentrations of the peak maxima could then be obtained for use in the Langmuir isotherm plots (see later). Proper detector wavelength selection also ensured reliable detector calibration.

Uracil was used as an unretained solute for determination of the column void volume, V_m. Polystyrene of molecular weight $1.8 \cdot 10^6$ was used with dichloromethane as mobile phase to measure the interstitial porosity, ε_0. Retention factors (k') were determined from the peak maxima of the large concentration bands. Apparent efficiency (N) was obtained using the width of the band at half-height ($W_{0.5}$) according to the equation

$$N = 5.54(t_R/W_{0.5})^2 \quad (1)$$

and following the guidelines of Golshan-Shirazi and Guiochon [16].

RESULTS AND DISCUSSION

It has been shown that for optimum productivity, the peparative liquid chromatographic technique should be operated under conditions of significant concentration overload such that peak overlap can occur [17]. Hence column efficiency can in large part be determined by the thermodynamic contribution (isotherm linearity) to band broadening rather then by axial dispersion and mass-transfer kinetics [1]. Under these conditions, optimization of the stationary phase characteristics in large-scale liquid chromatography is of interest.

In this paper, we examine the influence of stationary phase characteristics on the elution behavior of single-component (2-phenylethanol) bands of high concentration with mobile phases of $\leqslant 30\%$ aqueous methanol. First, we shall summarize measured characteristics of the packings used in this work. Second, various parameters (*i.e.*, injection size, k', flow-rate) are explored for a given system, followed by a study of the influence of C_{18}-bonded phase particle diameter and pore size. Lastly, Langmuir adsorption coefficients can be determined from the experimental data collected. These results should provide a further insight into the role of stationary phase properties in large-scale liquid chromatography.

Table I summarizes the stationary phases examined and their characteristics. Nitrogen BET surface areas of the sorbents and bonded-phase surface area per column are listed. Surface area is decreased by about 60% in the C_{18}-bonded 100 Å silica relative to the *ca.* 44% loss in the C_{18}-bonded 200 Å silica. The unbonded silicas show no micropores, so the decrease in surface area due to bonding affects the pores accessible to the solute. Thus, the *ca.* 50% excess surface-area advantage of the 100 Å silica is decreased to 15% owing to C_{18}-bonding and increased to about 30% after the sorbents have been packed into columns.

We also measured the interstitial volume, V_0, of each column by elution of

TABLE I

CHARACTERISTICS OF REVERSED-PHASES STUDIED

Stationary phase[a]	Surface area[b]			ε_0	ε_p	$\varepsilon_p/\varepsilon_0$	$\frac{\varepsilon_p}{1-\varepsilon_0}$
	Silica (m^2/g)	Bonded phase (m^2/g)	Bonded phase[c] (m^2)				
RG1010-C_{18}	366	152	170	0.44	0.24	0.55	0.43
RG1020-C_{18}	366	152	198	0.40	0.25	0.63	0.42
RG1040-C_{18}	385	160	192	0.38	0.26	0.68	0.42
RG1080-C_{18}	381	169	207	0.40	0.25	0.63	0.42
RG2010-C_{18}	246	139	163	0.44	0.36	0.82	0.64
RG2020-C_{18}	240	135	135	0.40	0.34	0.85	0.57

[a] The nomenclature RG_{xxyy}-C_{zz} indicates a silica of nominal *xx* nm pore diameter with *yy* μm particle diameter and bonded with C_{zz} alkyl chains. The C_{18} columns were 15 × 0.46 cm I.D.

[b] Surface area measured by the N_2 BET method.

[c] These values represented the total surface area in the column and are obtained from the bonded phase surface area and the packed density (g packing per column) of the column.

high-molecular-weight polystyrene in dichloromethane and the column pore volume, V_p, from the difference between V_0 and V_m, the column void volume (retention volume of uracil). V_0 and V_p are expressed as percentages of the empty column volume (*i.e.*, ε_0 and ε_p, respectively). The ε_0 value is roughly constant within experimental error (about 5% relative standard deviation) from column-to-column, reflecting a consistent packing procedure. Pore volume, ε_p, values however, increase by about 40% from the 100 Å to the 200 Å sorbent, reflecting less consumption of pore volume in the 200 Å silica by the C_{18} chains. Values for the ratio of pore volume to interstitial volume ($\varepsilon_p/\varepsilon_0$) and the fractional empty space of the particle [$\varepsilon_p/(1 - \varepsilon_0)$] are in agreement with the above results and the literature [18].

Effect of sample concentration

Fig. 1 summarizes the dependence of the apparent efficiency on sample load applied to the column containing 200 Å pore-size C_{18}-bonded silica of 20-μm particle diameter (*i.e.*, RG2020-C_{18} in Table I) with methanol–water (30:70) as mobile phase. Injections of 10 μl of 1–600 mg/ml (0.01–6 mg) 2-phenylethanol were injected onto the column and the resulting band widths measured. For solute concentrations $\leqslant$25 mg/ml, 2-phenylethanol is soluble in methanol–water (30:70) and volume overloading occurs at >250 μl injected for the solute peak at $k' = 5.3$ [19]. For concentrations >25 mg/ml, 2-phenylethanol is less soluble in methanol–water (30:70) and these solutions were made up in methanol. Large-volume injections of these solutions produced a significant V_m peak, possibly due to partial elution of the band. The 10-μl injections and variable-sized injections of 5, 10 and 25 mg/ml of 2-phenylethanol in methanol–water (30:70) produce a single curve with a plateau of about 1000 plates followed by a decrease in efficiency at higher loads. Increased and

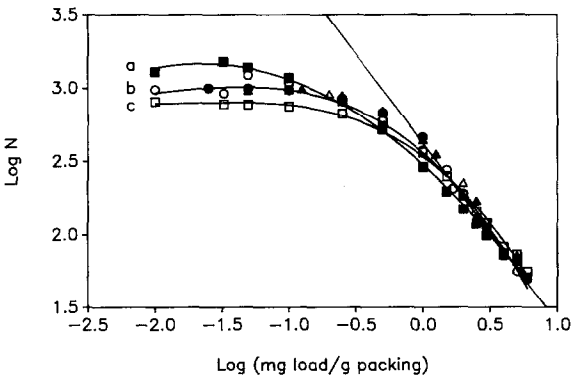

Fig. 1. Column efficiency as a function of 2-phenylethanol load on the RG2020-C_{18} column. A mobile phase of methanol–water (30:70, v/v) was used to obtain a k' of 5.3. A flow-rate of 1 ml/min was used, except where noted. ○ = 10-μl injections of variable concentration (1–600 mg/ml) 2-phenylethanol; ● = variable size injections (10–200 μl) of 5 mg/ml 2-phenylethanol; △ = variable size injections (10–200 μl) of 10 mg/ml 2-phenylethanol; ▲ = variable size injections (10–200 μl) of 25 mg/ml 2-phenylethanol; □ = 10-μl injections of 1–600 mg/ml 2-phenylethanol at a flow-rate of 1.5 ml/min; ■ = 10-μl injections of 1–600 mg/ml 2-phenylethanol at a flow-rate of 0.5 ml/min. (a) Curve through the ■ data points at flow-rate of 0.5 ml/min; (b) curve through the ○ data points at a flow-rate of 1 ml/min; (c) curve through the □ data points at a flow-rate of 1.5 ml/min.

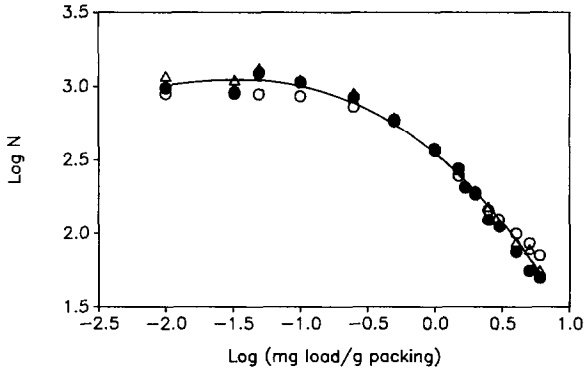

Fig. 2. Column efficiency as a function of 2-phenylethanol load at different k' values on the RG2020-C_{18} column. Injections of 10 μl of 1–600 mg/ml 2-phenylethanol were made into the column. Mobile phase composition of methanol–water adjusted to obtain the particular k' at a flow-rate of 1 ml/min. k': ○ = 2.3; ● = 5.2; △ = 9.3.

decreased volumetric flow-rates produce decreased (about 800 plates) and increased (1500 plates) efficiency, respectively, in the front half of the curve. The data points come together in the final portion of the curve to define a line of slope −1.1. This portion of the curve represents the greater contribution of isotherm non-linearity to the efficiency obtained in the system [16].

Fig. 2 shows data for efficiency *versus* load as a function of solute k' in the range 2–9. The points describe a single line with some scatter in the first part of the curve. The results in Figs. 1 and 2 are in good agreement with the literature [13,20].

Effect of particle diameter

We next studied the elution behavior of 2-phenylethanol on columns differing in particle size of the C_{18} 100 Å pore reversed-phase. Fig. 3 shows efficiency *versus* sample

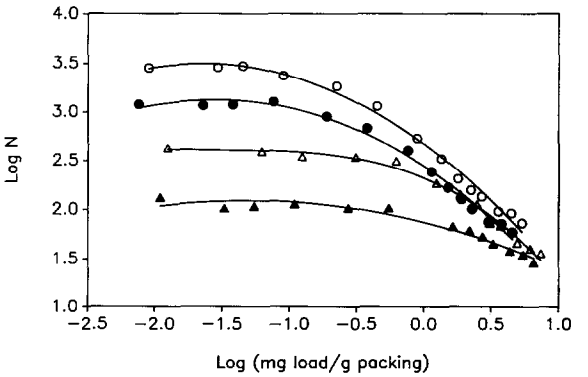

Fig. 3. Column efficiency as a function of 2-phenylethanol load for C_{18} columns of different particle diameter. Injections of 10 μl of 1–600 mg/ml 2-phenylethanol were made on each column operated with a methanol–water (30:70) eluent at 1 ml/min. ○ = RG1010-C_{18}, 10-μm particle diameter; ● = RG1020-C_{18}, 20 μm; △ = RG1040-C_{18}, 40 μm; ▲ = RG1080-C_{18}, 80 μm.

load for the four C_{18} sorbents of nominal particle diameter 10, 20, 40 and 80 μm. A mobile phase of methanol–water (30:70) was used to obtain an average solute k' of *ca.* 5.8 (4.5% relative standard deviation) in each system. The front portion of the

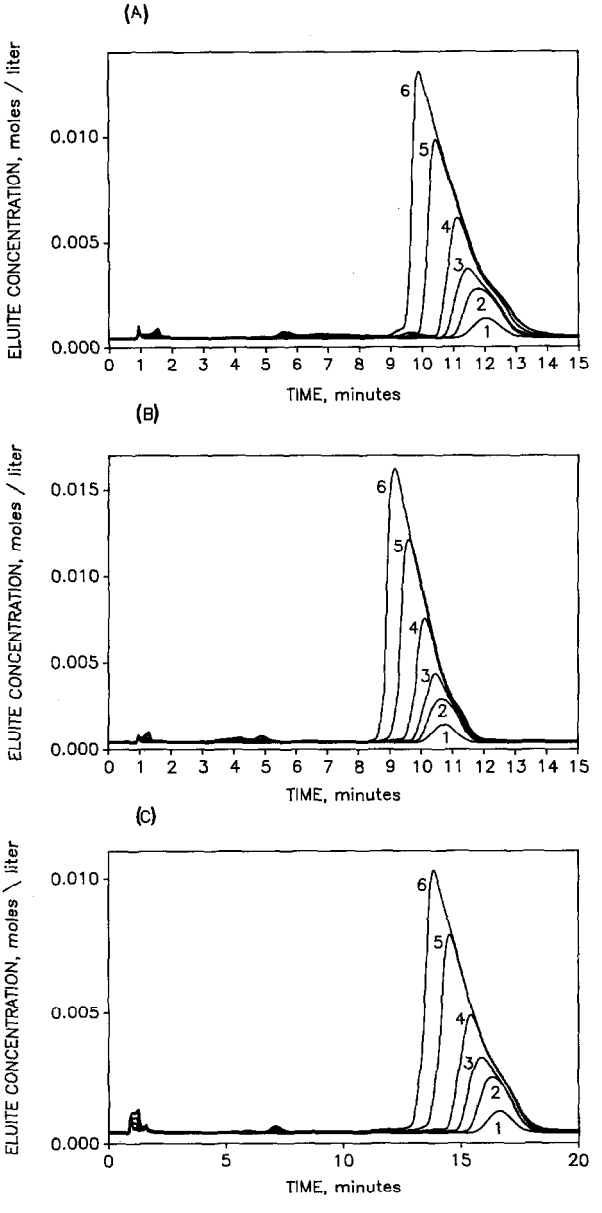

Fig. 4. Elution of high concentrations of 2-phenylethanol from C_{18} columns of different pore size. Each 15 × 0.46 cm I.D. column was operated at 1 ml/min. The chromatograms result from a 10-μl injection of the following 2-phenylethanol concentrations: 1 = 5 mg/ml (0.4 μmol solute injected); 2 = 25 mg/ml (2.0 μmol); 3 = 50 mg/ml (4.1 μmol); 4 = 100 mg/ml (8.2 μmol); 5 = 200 mg/ml (16.4 μmol); 6 = 300 mg/ml (24.6 μmol). (A) RG2020-C_{18}, k' = 5.3; (B) RG1020-C_{18}, k' = 5.4; (C) RG1020-C_{18}, k' = 8.9.

curves are determined by the efficiency of the column, *i.e.*, about $N = 3000$ plates for 10-μm, $N = 1000$ for 20-μm, $N = 425$ for 40-μm and $N = 130$ for 80-μm particles. The point at which the plots become non-linear at larger sample loads increases with increasing particle diameter. The slopes of the final portions of the curves are similar, with the exception of the 80-μm system, which still shows curvature. Although smaller particles always produced higher efficiency, beyond a certain sample load the rates of decrease in efficiency with load are similar. However, columns packed with smaller particles can be used at higher flow-rates with the advantage of a large production rate relative to the same efficiency obtained on the larger particle columns. Golshan-Shirazi and Guiochon [14] have detailed the optimization of efficiency via column length and particle size (d_p^2/L) and flow-rate compromises in a recent comprehensive study; the results of Fig. 3 are in agreement with these studies [8,13,20,21].

We now turn to a study of the influence of porosity on the efficiency/load behavior observed in Figs. 1–3.

Surface area effects

For this study, we examined 2-phenylethanol elution on four C_{18} reversed-phase columns: 10- and 20-μm particles in each of 100 and 200 Å pore sizes (RG1010-C_{18}, RG2010-C_{18}, RG1020-C_{18} and RG2020-C_{18} in Table I). The gain in surface area (based on nitrogen BET measurements) using the smaller pore-size packing is about 30% owing to the presence of C_{18} chains on the surface and the packed bed density in the column. The mobile phase conditions were adjusted to normalize k' to *ca.* 5 to examine in a straightforward manner the influence of increased pore diameter. In one case, methanol–water (30:70) was used to obtain 2-phenylethanol elution at $k' = 8.9$ and 5.3 on the RG1020-C_{18} and RG2020-C_{18} columns, respectively.

Fig. 4A–C show chromatograms for several sample loads of 2-phenylethanol on the 20-μm columns. In each chromatogram, the detector response at 254 nm was converted to solute concentration (M) in the mobile phase using the detector calibration graph constructed previously (see Experimental). Solute injections of 8 mM–2.5 M 2-phenylethanol solutions result in band elution with peak maxima of < 15 mM concentration in the mobile phase. For the same k', the 2-phenylethanol peak in the RG2020-C_{18} (200 Å) system shows slightly increased broadening and decreased retention at high load relative to the RG1020-C_{18} (100 Å) system. All of the chromatograms show peak tailing at high sample load, suggesting that a convex-shaped adsorption isotherm is operable. We have no explanation for the inflection point on the trailing side of the higher concentration peaks.

Fig. 5 details the efficiency–load relationship for the chromatograms in Fig. 4. In this plot we have not normalized sample load to mass of packing in the column. Plotting log N against log(mg sample load/g packing) yields curves for these data that are superimposed. Note that at the second data point (0.25 mg injected) in Fig. 5, the efficiency on the 200 Å system has decreased to 80% of the initial value relative to 95% of initial value for the 100 Å system. The points come together as the load is increased. Interestingly, increased k' on the RG1020-C_{18} column plays no role in the observed influence of sample load on efficiency.

One approach to studying the above experimental data is to apply the ideal and semi-ideal models developed for high solute concentration conditions by Golshan-

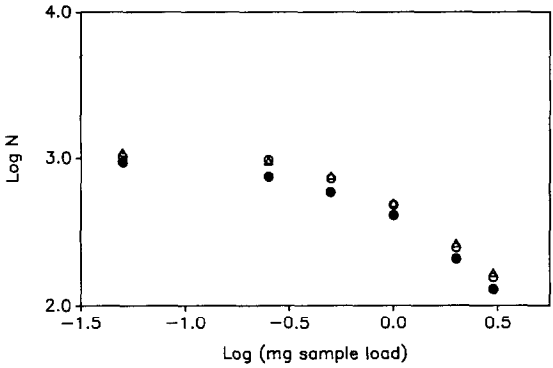

Fig. 5. Column efficiency as a function of 2-phenylethanol load on C_{18} columns. Conditions as in Fig. 4. ○ = RG1020-C_{18}, k' = 5.4; ● = RG2020-C_{18}, k' = 5.3; △ = RG1020-C_{18}, k' = 8.9.

Shirazi and Guiochon [16]. Using this approach, a loading factor, L_f, can be defined according the equation

$$L_f = \{1 - [(t_f - t_m - t_p)/(t_{R,0} - t_m)]^{0.5}\}^2 \quad (2)$$

where t_f is the retention time of the high concentration solute band, t_m the column void volume, t_p the injected pulse width and $t_{R,0}$ the retention time of a very small sample. Thus, L_f is proportional to k'_f/k'_0, *i.e.*, the decrease in band k' when the solute load is increased. Fig. 6 illustrates this relationship and shows that the 100 Å C_{18} sorbent provides less retention loss as the sample size increases relative to the larger pore size system. Note that even at larger values of L_f (*i.e.*, *ca.* 3%), the slopes of the curves are non-zero.

The plot of log N *vs.* log L_f in Fig. 7 shows a steeper slope for the RG1020-C_{18} system due not to a faster decrease in efficiency (see Fig. 5), but rather to a more

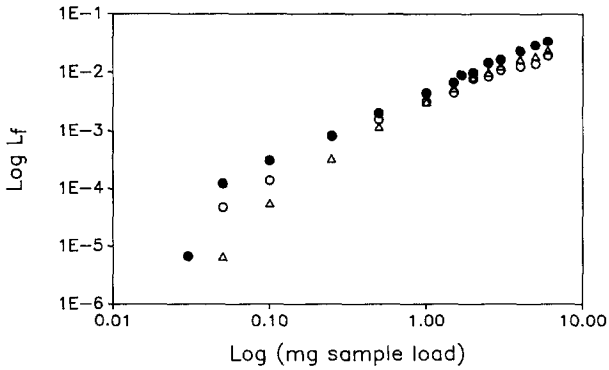

Fig. 6. Loading factor for 2-phenylethanol on C_{18} columns as a function of sample load. Conditions as in Fig. 4, except sample concentrations up to 600 mg/ml were investigated. Loading factor is defined in the text. ○ = RG1020-C_{18}, k' = 5.4; ● = RG2020-C_{18}, k' = 5.3; △ = RG1020-C_{18}, k' = 8.9.

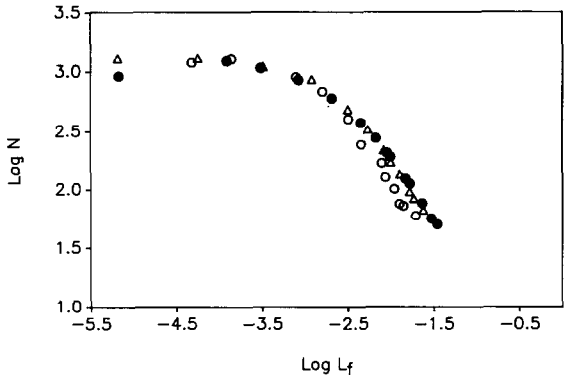

Fig. 7. Column efficiency as a function of loading factor for 2-phenylethanol on C_{18} columns. Conditions as in Fig. 4, except sample concentrations up to 600 mg/ml were investigated. Loading factor defined in the text. ○ = RG1020-C_{18}, k' = 5.4; ● = RG2020-C_{18}, k' = 5.3; △ = RG1020-C_{18}, k' = 8.9.

gradual change in L_f as sample size increases. From this point of view, the small pore size packing resists changes in k' (by virtue of a greater working surface area to accommodate solute) relative to the wider pore system. Employing the same solvent system as for k' = 5.3 on RG2020-C_{18} results in k' = 8.9 on RG1020-C_{18} and the resulting curve in Fig. 7 is shifted toward that for the wide-pore packing. This result reflects the dependence of L_f on solute load shown in Fig. 6 and is in agreement with the literature [16]. Similar conclusions can be drawn for the RG1010-C_{18} and RG2010-C_{18} systems.

Langmuir isotherm estimation

The L_f calculation and the chromatographic data at very small sample size provide a convenient means of calculating the coefficients of the Langmuir isotherm in accordance with the model of Golshan-Shirazi and Guiochon [16]. The Langmuir isotherm can be written as

$$Q = aC/(1 + bC) \tag{3}$$

where Q and C are the equilibrium concentrations of the solute in the stationary and mobile phases, respectively. The coefficient a is given by

$$a = \frac{(t_{R,0} - t_m)\varepsilon_T}{t_m(1 - \varepsilon_T)} \tag{4}$$

The total porosity, ε_T, is equal to $\varepsilon_0 + \varepsilon_p$, values of which are given in Table I. The coefficient b is defined as

$$b = \frac{L_f F(t_{R,0} - t_m)}{n_m} \tag{5}$$

TABLE II

LANGMUIR ISOTHERM CHARACTERISTICS OF C_{18} REVERSED-PHASES

All results obtained at $k' \approx 5$ except where noted.

Stationary phase	a	L_f (%)	b (l/M)	Q_{lim} (M)
RG1010-C_{18}	11.5	0.96	4.05	2.9
		1.87	3.94	
RG1020-C_{18}	12.3	1.26	4.14	2.9
		1.94	4.27	
RG1040-C_{18}	11.4	1.27	2.66	4.1
		1.70	2.85	
RG1080-C_{18}	11.2	1.69	2.74	4.1
		2.07	2.72	
RG2010-C_{18}	21.7	1.40	6.15	3.6
		2.78	6.08	
RG2020-C_{18}	15.4	1.47	7.22	2.2
		3.47	7.10	
RG1020-C_{18}[a]	27.0	0.98	10.6	3.1
		2.8	10.0	

[a] These results were obtained at $k' = 8.9$.

where F is the volumetric flow-rate and n_m the number of moles of solute injected. At high mobile phase solute concentration, C, the limiting stationary phase solute concentration, Q_{lim}, becomes equal to a/b, which in turn is proportional to n_m/V_s, where V_s is the volume of the stationary phase.

The assumption is made that the Langmuir equation can approximate the adsorption behavior of 2-phenylethanol in our studies. This assumption can be

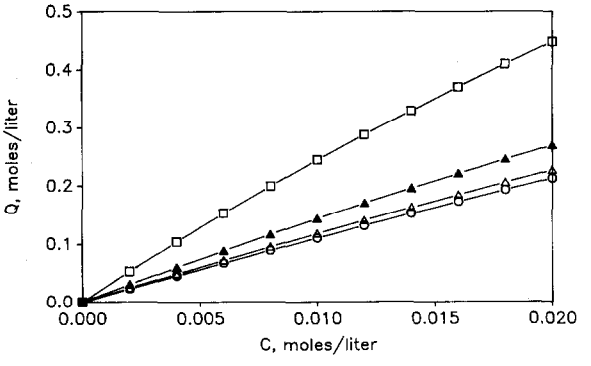

Fig. 8. Langmuir isotherm plot for 2-phenylethanol on C_{18} columns of different pore diameter. See text for explanation. ○ = RG1010-C_{18}, $k' = 5.6$; △ = RG1020-C_{18}, $k' = 6.1$; ▲ = RG2020-C_{18}, $k' = 5.5$; □ = RG1020-C_{18}, $k' = 8.9$.

checked by determining the constancy of b over several values of L_f [16]. Moreover, several studies using 2-phenylethanol in reversed-phase systems with methanol–water eluents utilized Langmuir isotherms for the description of solute adsorption [22,23].

Table II lists the a and b values for the columns studied, and Fig. 8 reconstructs selected isotherms over the mobile phase solute concentration used. The isotherms for the RG10 (100 Å) series differing in particle size were clustered together, as expected. For clarity, only the RG1010-C_{18} and RG1020-C_{18} curves are shown in Fig. 8. The RG2020-C_{18} plot lies above the 100 Å curves. Increasing k' to *ca.* 9 causes the isotherm for the RG1020-C_{18} column to rise above that for the RG10 system at $k' = 5$ and the 200 Å column. In the mobile phase solute concentration range studied in Fig. 8, the isotherm equation is dominated by a. In turn, a is influenced greatly by the total porosity of the system, *i.e.*, increasing ε_T from 0.65 to 0.8 increases a from 9.3 to 20 for a fixed k' of 5.0. Hence the C_{18} chains serve to modulate the effect of decreased pore diameter (*i.e.*, greater surface area) because they occupy a greater portion of the pore volume. Preliminary results suggest a 100 Å C_4-bonded phase can produce a larger a value owing to an increased ε_T, assuming that the mobile phase can be manipulated to achieve comparable retention. The limiting stationary phase solute concentration is shown in Table II as Q_{lim} and is in the range 2–4 M. On average, Q_{lim} is lower in the RG20 columns and reflects the decreased bonded-phase surface area in this system (see Table I).

CONCLUSIONS

We have examined the loading behavior of 2-phenylethanol in methanol–water eluents on C_{18} reversed-phase columns differing in particle size and pore size. As the solute concentration at a fixed injection volume onto the column is increased, the apparent efficiency at first remains constant and then decreases. The onset of efficiency loss depends on the magnitude of the initial column efficiency. In these studies, larger particles (*e.g.*, 80 μm) maintained their efficiency over a wider range of solute load relative to smaller particles (*e.g.*, 10 μm). Of course, the 10-μm column always provided more plates than the 80-μm column. Retention factors in the range 2–9 did not influence the dependence of efficiency on solute load. The loading factor, L_f, proportional to the decrease in band k' when the sample load was increased, showed a dependence on the pore size of the C_{18} sorbent used. Using the retention time method of Golshan-Shirazi and Guiochon [16], plots of efficiency *versus* loading factor reveal that the small-pore (100 Å) C_{18} sorbents showed slightly greater efficiency and less loss in k' as the solute load is increased relative to the large-pore (200 Å) C_{18} stationary phase. Langmuir isotherm coefficients could be estimated from the experimental data for the adsorption of 2-phenylethanol in these systems. The a value plays a dominant role in the range of mobile phase solute concentrations studied and is greatly affected by the total porosity of the column. Separate measurements of bonded-phase surface area and column pore volume revealed that the C_{18} bonding on 100 Å silica consumes proportionately more (about 60%) pore volume than on the 200 Å silica (*ca.* 44% consumed), and serves to diminish the advantageous higher surface area of the small-pore silica.

ACKNOWLEDGEMENTS

This paper is dedicated to Dr. Lloyd R. Snyder on the occasion of his sixtieth birthday.

The author thanks J. T. Kowalewski for the packing of several columns and B. P. Wilson for assistance with the chromatographic experiments. M. R. Derolf is thanked for numerous valuable discussions.

REFERENCES

1 J. H. Knox and H. M. Pyper, *J. Chromatogr.*, 363 (1986) 1.
2 A. Jaulmes, C. Vidal-Madjar, H. Colin and G. Guiochon, *J. Phys. Chem.*, 90 (1986) 207.
3 J. E. Eble, R. L. Grob, P. E. Antle and L. R. Snyder, *J. Chromatogr.*, 384 (1987) 25.
4 Cs. Horváth, A. Nahum and J. H. Frenz, *J. Chromatogr.*, 218 (1981) 365.
5 F. Eisenbeiss, S. Ehlevding, A. Wehrli and J. F. K. Huber, *Chromatographia*, 20 (1985) 657.
6 H. Poppe and J. C. Kraak, *J. Chromatogr.*, 255 (1983) 395.
7 G. Cretier and J. L. Rocca, *Chromatographia*, 20 (1985) 461.
8 J. Newburger, L. Liebes, H. Colin and G. Guiochon, *Sep. Sci. Technol.*, 22 (1987) 1933.
9 S. Golshan-Shirazi and G. Guiochon, *J. Phys. Chem.*, 93 (1989) 4341.
10 L. R. Snyder, G. B. Cox and P. E. Antle, *Chromatographia*, 24 (1987) 82.
11 J. N. Little, R. L. Cotter, J. A. Prendergast and P. D. McDonald, *J. Chromatogr.*, 126 (1976) 439.
12 H. Colin, P. Hilaireau and J. de Tournemire, *LC · GC*, 8 (1990) 302.
13 A. W. J. De Jong, H. Poppe and J. C. Kraak, *J. Chromatogr.*, 209 (1981) 432.
14 S. Golshan-Shirazi and G. Guiochon, *Anal. Chem.*, 61 (1989) 1368.
15 S. Golshan-Shirazi, S. Ghodbane and G. Guiochon, *Anal. Chem.*, 60 (1988) 2630.
16 S. Golshan-Shirazi and G. Guiochon, *Anal. Chem.*, 61 (1989) 462.
17 A. Katti and G. Guiochon, *Anal. Chem.*, 61 (1989) 982.
18 B. W. Sands, Y. S. Kim and J. L. Bass, *J. Chromatogr.*, 360 (1986) 353.
19 P. Gareil and R. Rosset, *J. Chromatogr.*, 450 (1988) 13.
20 H. Colin, *Sep. Sci. Technol.*, 22 (1987) 1851.
21 S. Golshan-Shirazi and G. Guiochon, *Anal. Chem.*, 60 (1988) 2364.
22 Z. Ma, A. Katti, B. Lin and G. Guiochon, *J. Phys. Chem.*, 94 (1990) 6911.
23 G. B. Cox and L. R. Snyder, *J. Chromatogr.*, 483 (1989) 95.